

This discussion paper is/has been under review for the journal Biogeosciences (BG).
Please refer to the corresponding final paper in BG if available.

Inverse estimation of source parameters of oceanic radioactivity dispersion models associated with the Fukushima accident

Y. Miyazawa, Y. Masumoto, S. M. Varlamov, T. Miyama, M. Takigawa, M. Honda, and T. Saino

Research Institute for Global Change, Japan Agency for Marine-Earth Science and Technology, Yokohama, Kanagawa, Japan

Received: 3 September 2012 – Accepted: 2 October 2012 – Published: 11 October 2012

Correspondence to: Y. Miyazawa (miyazawa@jamstec.go.jp)

Published by Copernicus Publications on behalf of the European Geosciences Union.

BGD

9, 13783–13816, 2012

Inverse estimation of source parameters of oceanic radioactivity dispersion models

Y. Miyazawa et al.

Title Page

Abstract

Introduction

Conclusions

References

Tables

Figures

⏪

⏩

◀

▶

Back

Close

Full Screen / Esc

Printer-friendly Version

Interactive Discussion

Abstract

With combined use of the ocean-atmosphere simulation models and field observation data, we evaluate the parameters associated with the total caesium-137 amounts of the direct release into the ocean and atmospheric deposition over the Western North Pacific caused by the accident of Fukushima Daiichi nuclear power plant (FNPP) that occurred in March 2011. The Green's function approach is adopted for the estimation of two parameters determining the total emission amounts for the period from 12 March to 6 May 2011. It is confirmed that the validity of the estimation depends on the simulation skill near FNPP. The total amount of the direct release is estimated as $5.5\text{--}5.9 \times 10^{15}$ Bq, while that of the atmospheric deposition is estimated as $5.5\text{--}9.7 \times 10^{15}$ Bq, which indicates broader range of the estimate than that of the direct release owing to uncertainty of the dispersion widely spread over the Western North Pacific.

1 Introduction

Radionuclides associated with the accident of Fukushima Daiichi nuclear power plant (FNPP) that occurred in March 2011 seriously contaminated the ocean around FNPP as reported by Nuclear Emergency Response Headquarters (NERH, 2011). There exist two major sources of the ocean contamination (NERH, 2011): direct release from FNPP into the ocean (Kawamura et al., 2011; Tsumune et al., 2012; Bailly du Bois et al., 2011; Masumoto et al., 2012; Miyazawa et al., 2012) and atmospheric deposition (Takemura et al., 2011; Kawamura et al., 2011; Morino et al., 2011; Honda et al., 2012; Stohl et al., 2012; Aoyama et al., 2012a, b). Other sources including indirect release from groundwater, river discharge water, or coastal sediment supply the nuclides into the ocean for the long time period (Buesseler et al., 2011; Oura and Ebihara, 2012). The two major sources, however, dominantly drove the oceanic dispersion during the initial period from March to May 2011 and basically determined the total amount of the

BGD

9, 13783–13816, 2012

Inverse estimation of source parameters of oceanic radioactivity dispersion models

Y. Miyazawa et al.

Title Page

Abstract

Introduction

Conclusions

References

Tables

Figures

⏪

⏩

◀

▶

Back

Close

Full Screen / Esc

Printer-friendly Version

Interactive Discussion

radionuclides emission into the ocean (Kawamura et al., 2011; Tsumune et al., 2012; Aoyama et al., 2012a).

Kawamura et al. (2011) evaluated 4×10^{15} Bq (4 PBq) of the total amount of caesium-137 (^{137}Cs) directly released into the ocean for the period from 21 March to 30 April 2011 using their numerical ocean model and the observations in front of FNPP. Tsumune et al. (2012) also evaluated 3.5 ± 0.7 PBq of the ^{137}Cs amount for the period from 26 March to 30 May 2011 based on the similar method. Several numerical simulations of the ^{137}Cs dispersion show some similarity and difference among them (Masumoto et al., 2012). It is useful and necessary to evaluate the total amount of direct release using different models based on different methods for better understanding to uncertainty involved in this kind of estimations.

The total amount of the atmospheric deposition over the ocean was also evaluated using numerical model simulations with combined use of the field observation data by several groups: e.g. 5 PBq for the period from 12 March to 30 April 2011 (Kawamura et al., 2011). The atmospheric deposition effectively transported the radionuclides over the North Pacific during the initial period (Honda et al., 2012; Aoyama et al., 2012b). Using an output of the atmospheric dispersion model, our previous study (Honda et al., 2012) suggested that the anomalous ^{137}Cs concentration measured at a point far from FNPP (47° N, 160° E) on 21 April 2011, just after one month of the Fukushima accident, was actually caused by the atmospheric deposition. We also suggested that the total deposition amount of our previous model (0.18 PBq within March 2011) was much lower than the other estimate of 5 PBq (Kawamura et al., 2011) even though both the models used the same source information (Chino et al., 2011). The difference could come from the large uncertainty of the fallout to the parameterizations of the wet and dry deposition processes (Stohl et al., 2012).

In this study, we estimate the total ^{137}Cs amounts of the direct release and atmospheric deposition on the sea originating from FNPP during the initial period from 12 March to 6 May 2011 by using the outputs from numerical ocean-atmosphere models and all available field observation data. For this we adopt the Green's function approach

BGD

9, 13783–13816, 2012

Inverse estimation of source parameters of oceanic radioactivity dispersion models

Y. Miyazawa et al.

Title Page

Abstract

Introduction

Conclusions

References

Tables

Figures

⏪

⏩

◀

▶

Back

Close

Full Screen / Esc

Printer-friendly Version

Interactive Discussion

dispersion model (Honda et al., 2012),

$$K_v \frac{\partial C}{\partial z} = D_a^f(x, y, t) \quad (2)$$

where K_v is the vertical diffusion coefficient. The information of ^{137}Cs direct release from FNPP is included by a flux term indicated by the fourth term of the right-hand side. $\delta(x_0, y_0, z_0)$ is 1 only at a surface source grid in front of FNPP and is 0 at all other grids. $D_o(t)$ denotes a function of ^{137}Cs direct release flux from FNPP. We use grid coordinates and ocean currents provided from two different ocean general circulation models: JCOPE2 (Miyazawa et al., 2009) and JCOPE-T (Guo et al., 2010; Miyazawa et al., 2012) to examine sensitivity of simulation results on possible model biases. Note that Eq. (1) does not involve the sediment and biological processes (Masumoto et al., 2012) though their roles are non-negligible especially for the whole ^{137}Cs dispersion process on long time scale.

A basin-scale model JCOPE2 (Miyazawa et al., 2009) developed based on Princeton Ocean Model with generalized coordinate of sigma (Mellor et al., 2002) provides daily mean ocean current data covering the Western North Pacific (10.5–62° N, 108–180° E) with horizontal resolution of 1/12°. The main objective of JCOPE2 is a description of the observed oceanic variability associated with the Kuroshio, Kuroshio-Extension, Oyashio, and mesoscale eddies around Japan. The JCOPE2 model thus assimilates the remote-sensing data of altimetry and surface temperature and in-situ data of temperature and salinity profiles. Surface momentum and heat fluxes are calculated by using the bulk formulae (Kagimoto et al., 2008) with atmospheric variables obtained from the National Centers for Environmental Prediction/National Center for Atmospheric Research (NCEP/NCAR) reanalysis (Kalnay et al., 1996). Sea surface salinity flux is represented by a relaxation term to monthly climatological data of sea surface salinity (Conkright et al., 2002).

The JCOPE-T model (Guo et al., 2010; Miyazawa et al., 2012) is a downscaled version of JCOPE2 and provides hourly data of ocean current covering the Japan coastal

Inverse estimation of source parameters of oceanic radioactivity dispersion models

Y. Miyazawa et al.

Title Page

Abstract

Introduction

Conclusions

References

Tables

Figures

⏪

⏩

◀

▶

Back

Close

Full Screen / Esc

Printer-friendly Version

Interactive Discussion



ocean (28–44° N, 125–148° E) with horizontal resolution of 1/36°. The lateral boundary condition is given by the JCOPE2 model. The observed features of mesoscale phenomena are represented by nudging of temperature and salinity toward the JCOPE2 data. Most significant difference between JCOPE2 and JCOPE-T is that the latter (former) model includes (no) explicit tidal forcing. Tidal forcing composed of 16 constituents is included in JCOPE-T by additions of equivalent surface pressure gradient. The tidal velocity and sea level anomaly provided from a tide model (Matsumoto et al., 2000) are also specified at lateral boundaries. Another feature of JCOPE-T different from JCOPE2 is inclusion of lateral fresh water inputs from 35 major river mouths including the Kitakami and Abukuma rivers near FNPP (Fig. 1b). Surface fluxes of momentum, heat, and fresh water are calculated using sophisticated algorithms (Li et al., 2010) with hourly data of atmospheric variables obtained from Japan Meteorological Agency non-hydrostatic Meso Scale Model (JMA MSM; Saito et al., 2007), which has much higher horizontal resolution of 5 km as compared to a few hundred km resolution of the NCEP/NCAR reanalysis data used for the JCOPE2 model. The JCOPE-T current was also used for a dispersion simulation described in our previous studies (Masumoto et al., 2012; Miyazawa et al., 2012). The present version of JCOPE-T (JCOPE-T-2) is slightly modified by changing the time scale of the nudging toward the JCOPE2 temperature and salinity from 20-day over the whole region to 5-day in the open ocean with water depth larger than 200 m. In addition, the nudging of the present model is removed in the shallow region with water depth smaller than 200 m. The modification of the nudging time scale actually improved the biases of intensification of Oyashio and relevant southward deviation of the latitudinal position of Kuroshio Extension (e.g. see Fig. 3 in Masumoto et al., 2012) found in the previous version of JCOPE-T (JCOPE-T-1).

Distributions of surface currents averaged for the simulation period (Fig. 1) indicate that the southward current associated with the Oyashio intrusion is represented in open ocean with bottom depth larger than 200 m by both JCOPE2 (Fig. 1a) and JCOPE-T-2 (Fig. 1b). An anticyclonic eddy near the coast south of 37° N is also represented by

Inverse estimation of source parameters of oceanic radioactivity dispersion models

Y. Miyazawa et al.

[Title Page](#)[Abstract](#)[Introduction](#)[Conclusions](#)[References](#)[Tables](#)[Figures](#)[Back](#)[Close](#)[Full Screen / Esc](#)[Printer-friendly Version](#)[Interactive Discussion](#)

both models. The northeastward flow of the Kuroshio Extension is reproduced around 36.8° N in JCOPE2 as reported in the Quick Bulletin of oceanographic conditions provided from Japan Coast Guard but it is not shown around this latitude in JCOPE-T-2, indicating a remaining southward bias of the Kuroshio Extension front position in this version of JCOPE-T-2. River discharges flows from two major rivers near FNPP (the Kitakami and Abukuma rivers) are represented in JCOPE-T-2.

Atmospheric deposition of ^{137}Cs is estimated by a one-way nested regional air quality forecasting (AQF) system described by Honda et al. (2012). The model domain covers the Western Pacific with a horizontal resolution of 10 km. Source information of ^{137}Cs is given by a scenario of ^{137}Cs emission from the FNPP created by combined use of the SPEEDI reverse method (Chino et al., 2011) and data in Tokyo Electric Power Corporation (TEPCO) reports (Honda et al., 2012). The system is driven by meteorological data from the NCEP operational global analysis data set. Wet and dry deposition schemes used in AQF are based on Maryon et al. (1996). Three significant peaks of atmospheric deposition integrated over the Western North Pacific (10.5–62° N, 108–180° E) are depicted in the time sequence (Fig. 2). Total amount of the atmospheric deposition in the Western North Pacific for the period from 11 March to 6 May 2011 is 0.3 PBq. Horizontal distribution of the accumulated deposition is depicted in Honda et al. (2011)'s Fig. 3.

2.2 Observation data

To adjust model parameters associated with the emission amounts, we utilize two kinds of observation data: (1) data of urgent monitoring by TEPCO and Ministry of Education, Culture, Sports, Science and Technology (MEXT) with relatively large values of measurement uncertainty and detection limit, and (2) more precise data obtained by research cruises of R/Vs *Tansei*, *Mirai* and volunteer ships managed by NYK LINE (Table 1 for detail). Spatial sampling density is higher in the former types of data measured near FNPP than in the latter types of data measured far from it (Fig. 3). Table 1

BGD

9, 13783–13816, 2012

Inverse estimation of source parameters of oceanic radioactivity dispersion models

Y. Miyazawa et al.

Title Page

Abstract

Introduction

Conclusions

References

Tables

Figures

⏪

⏩

◀

▶

Back

Close

Full Screen / Esc

Printer-friendly Version

Interactive Discussion

summarizes the information of the observation data used in this study. Note that data showing no detection of ^{137}Cs are excluded from our analysis.

3 First guess simulations

A first guess of the direct release flux term $D_o^f(t)$ is evaluated using the daily observation data of ^{137}Cs near the FNPP as following,

$$D_o^f(t) = \frac{(C_{\text{grid}} \cdot C_{\text{obs}} - C(x_0, y_0, z_0, t))}{T_s} \quad (3)$$

where C_{obs} and $C(x_0, y_0, z_0, t)$ denote an average of two observed concentrations in front of FNPP (the 5th–6th and south discharge canal waters; Tsumune et al., 2012) and simulated concentration at the source grid, respectively. Magnitude of the flux is determined by a relaxation time scale T_s , which is assumed to be 36-h in this study. C_{grid} denotes a constant for adjustment of a grid size effect, which equals $1/9$ in the simulation using the JCOPE2 grid ($1/12^\circ$) but equals 1 in the JCOPE-T simulations with the $1/36^\circ$ grid to allow similar levels of total emission amount between the JCOPE2 and JCOPE-T simulations. To estimate the first guess flux of direct release, we perform two base simulations using the JCOPE-T-1 and JCOPE2 current data without the atmospheric deposition. Note that the JCOPE-T-2 current data were calculated after the derivation of the JCOPE-T-1 flux, which may not be much different from the flux based on the JCOPE-T-2 current data. We thus decide to use the JCOPE-T-1 flux for both the JCOPE-T-1 and JCOPE-T-2 cases.

Time sequences of calculated direct release fluxes (Fig. 4) show two peaks of significant emission during the period from the end of March to the beginning of April. Total amounts of estimated direct release for the period from 21 March to 6 May are 1.9 PBq for JCOPE-T-1 and 1.6 PBq for JCOPE2. Slight larger amount evaluated in the JCOPE-T-1 flux as compared to the JCOPE2 flux suggests effective ^{137}Cs transport

BGD

9, 13783–13816, 2012

Inverse estimation of source parameters of oceanic radioactivity dispersion models

Y. Miyazawa et al.

Title Page

Abstract

Introduction

Conclusions

References

Tables

Figures

⏪

⏩

◀

▶

Back

Close

Full Screen / Esc

Printer-friendly Version

Interactive Discussion



from the source grid to surrounding region in the JCOPE-T-1 simulation due to its more energetic ocean current variation around FNPP (not shown).

We use another type of the flux $D_o^f(t)$ proposed by a research group of Japanese Central Research Institute of Electric Power Industry (CRIEPI) whose time sequence is also shown in Fig. 4. We call this type of flux the CRIEPI flux with total release amount of 3.5 PBq (Tsumune et al., 2012). Note that the CRIEPI (JCOPE-T-1 and JCOPE2) flux assumes the direct release started from 26 (21) March 2011 (see Fig. 4). However, the release amount for the period from 21 to 25 March 2011 estimated in the JCOPE-T-1 and JCOPE2 fluxes is not so large as compared to that for the later period.

Five cases of the first guess simulations used for the inverse estimation are summarized in Table 2. Ocean current data includes JCOPE-T-1 with horizontal resolution of $1/36^\circ$, JCOPE-T-2 with $1/36^\circ$, and JCOPE2 with $1/12^\circ$. Three types of the direct release flux: JCOPE-T, JCOPE2, and CRIEPI are adopted. All first guess simulations specify zero atmospheric deposition flux. To compare level of agreement between the simulations and observation, we calculate values of a cost function

$$C = (\mathbf{y} - \mathbf{x}^f - \mathbf{x}^b)^t \mathbf{R}^{-1} (\mathbf{y} - \mathbf{x}^f - \mathbf{x}^b), \quad (4)$$

where $\mathbf{x}^f = (x_1^f, \dots, x_N^f)^t$ and $\mathbf{y} = (y_1^o, \dots, y_N^o)^t$ denote N -number concentration values of the simulation and observation, respectively; $\mathbf{x}^b = (0.001 \text{ Bq l}^{-1}, \dots, 0.001 \text{ Bq l}^{-1})^t$ are the background ^{137}Cs concentration (Aoyama et al., 2012b); \mathbf{R} denotes a $N \times N$ observation error covariance matrix whose diagonal components are specified from the measurement errors described in Table 1. Non-diagonal components of \mathbf{R} are all zero.

The JCOPE2 simulation shows the largest cost value that is significantly larger than all other simulations of the finer grid, suggesting that a coarse resolution of the model ($1/12^\circ$) is insufficient to represent observed ^{137}Cs variations. A larger total amount of the direct release flux represent by the CRIEPI flux results in smaller values of the cost function than those evaluated using the JCOPE-T-1 fluxes with the smaller total amount, indicating that the total direct release amount may be larger than 1.9 PBq of the JCOPE-T-1 flux total amount.

Inverse estimation of source parameters of oceanic radioactivity dispersion models

Y. Miyazawa et al.

Title Page

Abstract

Introduction

Conclusions

References

Tables

Figures



Back

Close

Full Screen / Esc

Printer-friendly Version

Interactive Discussion



Inverse estimation of source parameters of oceanic radioactivity dispersion models

Y. Miyazawa et al.

Title Page

Abstract

Introduction

Conclusions

References

Tables

Figures

⏪

⏩

◀

▶

Back

Close

Full Screen / Esc

Printer-friendly Version

Interactive Discussion



Figure 5 shows a sequence of weekly mean concentration calculated by the first guess JCOPE-T-2-C simulation that has a best fitting to the observation as a result of the parameters estimation (Table 3) described in Sect. 4. The horizontal dispersion process inside of the shelf is basically governed by the wind forced current (Tsumune et al., 2012; Miyazawa et al., 2012). The dispersion is limited near the coast within March 2011 (Fig. 5a, b). Then the dispersion elongates toward the northeastward direction in April (Fig. 5c–f). A change of dominant wind direction from northerly and/or easterly to southerly and/or westerly accounts for that of the dominant dispersion direction (Miyazawa et al., 2012). Figure 5 also indicates that the concentration measured along 141.4° E is basically underestimated by the first guess simulation. The atmospheric deposition and/or underestimation of the direct release may be responsible for the disagreement between the first guess simulation and observation.

4 Inverse estimation of source parameters

The first guess simulations suggest that the absolute levels of the simulated ^{137}Cs concentration could be adjusted based on comparison of the simulated and observed concentration values. We estimate two simple scaling factors (S_a , hereafter, the atmospheric parameter, and S_o , hereafter, the ocean parameter) for the adjustment of the atmospheric deposition

$$K_v \frac{\partial C}{\partial z} = (O_a + S_a) D_a^f(x, y, t) \quad (5)$$

and direct release fluxes

$$D_o(t) = (O_o + S_o) D_o^f(t) \quad (6)$$

where $O_a = 0$ and $O_o = 1$ are original values of the atmospheric and ocean parameters, respectively.

The Green's function approach (Menemenlis et al., 2005) is effective for the parameters estimation since it enables us to take account of error covariance among different parameters. N numbers of observation values \mathbf{y} are approximated using the Green's function: $\mathbf{y} = \mathbf{G}\Delta\boldsymbol{\eta} + \mathbf{x}^f + \mathbf{x}^b + \boldsymbol{\varepsilon}$, where $\Delta\boldsymbol{\eta} = \begin{pmatrix} S_a \\ S_o \end{pmatrix}$ and $\boldsymbol{\varepsilon}$ denote the errors of the estimation: $\boldsymbol{\varepsilon} = (\varepsilon_1, \dots, \varepsilon_N)^t$. The green's function

$$\mathbf{G} = \begin{pmatrix} G_{11} & G_{12} \\ \vdots & \vdots \\ G_{N1} & G_{N2} \end{pmatrix} \quad (7)$$

is calculated from results of parameters sensitivity experiments as following:

$$G_{n1} = (x_n^a - x_n^f)/S_a^1 \quad \text{and} \quad G_{n2} = (x_n^o - x_n^f)/S_o^1 (n = 1, \dots, N), \quad (8)$$

where x_n^a and x_n^o are ^{137}Cs concentrations corresponding to the n th observation calculated by the sensitivity experiments for the atmospheric deposition with perturbed parameter of S_a^1 and direct release with S_o^1 , respectively. Optimized parameters to minimize a cost function $\boldsymbol{\varepsilon}^t \mathbf{R}^{-1} \boldsymbol{\varepsilon}$ are obtained as

$$\Delta\boldsymbol{\eta}^0 = \mathbf{P}\mathbf{G}^t \mathbf{R}^{-1} (\mathbf{y} - \mathbf{x}^f - \mathbf{x}^b), \quad \mathbf{P} = (\mathbf{G}^t \mathbf{R}^{-1} \mathbf{G})^{-1}, \quad (9)$$

where \mathbf{R} and \mathbf{P} represent an error covariance matrix of the observations and parameters, respectively. We assume that the observation error covariance matrix \mathbf{R} is diagonal with the variance calculated from measurement errors mentioned in Sect. 2.2. Since the model linearly responses to the perturbations of the flux parameters shown in Eqs. (5) and (6), we expect that the Green's function approach works well for the parameters optimization (Menemenlis et al., 2005).

We conduct two sensitivity experiments perturbing the atmospheric ($S_a = 2$) and ocean ($S_o = 1$) parameters for each first guess simulation. Note that we exclude observations obtained two points in front of FNPP (the 5th–6th and south discharge canal

Inverse estimation of source parameters of oceanic radioactivity dispersion models

Y. Miyazawa et al.

Title Page

Abstract

Introduction

Conclusions

References

Tables

Figures

⏪

⏩

◀

▶

Back

Close

Full Screen / Esc

Printer-friendly Version

Interactive Discussion



waters) from Eqs. (4) and (9) because the horizontal grids of our models: $1/36^\circ$ and $1/12^\circ$ may be too coarse to represent the ^{137}Cs variation in front of FNPP. The optimization results based on the five cases of the first guess simulations are summarized in Table 3. The cost function value expected in the case with the optimized parameters (the expected cost) is calculated as

$$C_G = (\mathbf{y} - \mathbf{x}^f - \mathbf{G}\Delta\boldsymbol{\eta}^o - \mathbf{x}^b)^t \mathbf{R}^{-1} (\mathbf{y} - \mathbf{x}^f - \mathbf{G}\Delta\boldsymbol{\eta}^o - \mathbf{x}^b) \quad (10)$$

Optimizations of multiple parameters for the direct release and atmospheric deposition (see second and third columns of Table 3) generally exhibit more reduction of the expected cost values than optimizations for either single parameter (see fourth and fifth columns of Table 3). The errors of the parameters estimation are represented in the diagonal components of the error covariance matrix \mathbf{P} (Menemenlis et al., 2005; also see Eq. 9). The orders of the errors are $O(10^{-3})$ and $O(10^{-2})$ PBq for the direct release and atmospheric deposition, respectively, and are much smaller than the differences of $O(10^{-1}) - O(1)$ PBq among the estimates for different ocean currents and first guess direct release fluxes, as shown in Table 3.

5 Discussion

The optimization for the multiple parameters using the coarse grid model JCOPE2 fails to the estimation of the realistic amount of the atmospheric deposition, which is evaluated as a negative value (Table 3). To examine the failed estimation process in detail, we calculate contribution rates C_{nm}^r (in %; $m = 1, 2$) of the each measurement for the parameters estimation,

$$C_{mn}^r = [\mathbf{PG}^T]_{mn} [\mathbf{R}^{-1} (\mathbf{y} - \mathbf{x}^f - \mathbf{x}^b)]_n \frac{100}{|[\Delta\boldsymbol{\eta}^o]_m|}, \quad (11)$$

where $[\dots]_{mn}$ and $[\dots]_{n(m)}$ denote components of a matrix and a vector, respectively. The contribution rates C_{nm}^r are useful to distinguish contribution of an observation y_n^o for

BGD

9, 13783–13816, 2012

Inverse estimation of source parameters of oceanic radioactivity dispersion models

Y. Miyazawa et al.

Title Page

Abstract

Introduction

Conclusions

References

Tables

Figures

◀

▶

◀

▶

Back

Close

Full Screen / Esc

Printer-friendly Version

Interactive Discussion



the optimized parameter perturbation $[\Delta\eta^{\circ}]_m$, as suggested by the following equation:

$$100 \times \frac{[\Delta\eta^{\circ}]_m}{|[\Delta\eta^{\circ}]_m|} = \sum_{n=1}^N [\mathbf{P}\mathbf{G}^T]_{mn} [\mathbf{R}^{-1}(\mathbf{y} - \mathbf{x}^f - \mathbf{x}^b)]_n \frac{100}{|[\Delta\eta^{\circ}]_m|} = \sum_{n=1}^N C_{mn}^r \quad (12)$$

Figure 6 compares the contribution rates of JCOPE-T-2-C (upper panels), which has the smallest cost function value, and JCOPE2 (lower panels), which has the largest cost function value (Table 3). The unrealistic negative perturbation of the atmospheric parameter in the JCOPE2 case is caused by the adjustment to the observations near the coast and one observation around 36° N, 146° E (Fig. 6A-2), while almost all observations force positive perturbation of the atmospheric parameter in the JCOPE-T-2-C case (Fig. 6A-1). The negative perturbation of the atmospheric parameter shown near the coast (Fig. 6A-2) seems to be compensated by the positive perturbation of the ocean parameter there (Fig. 6O-2). The worst representation skill of JCOPE2 indicated by the largest cost function value (Table 2) is mainly attributed to the model performance near the coast (not shown). The negative perturbation of the atmospheric parameter in the JCOPE2 case could come partly from the worse simulation skill near the coast.

Another part of observation associated with the negative perturbation of the atmospheric parameter around 36° N, 146° E contributes to decrease the ocean parameter (Fig. 6O-2). Comparison between the concentration maps of JCOPE-T-2-C and JCOPE2 with only the direct release flux in the last week of April 2011 (Fig. 7) indicates that the coarser grid of JCOPE2 results in more diffusive horizontal dispersion as compared to JCOPE-T-2-C with the finer grid. The diffusive dispersion of JCOPE2 facilitates to transport more amount of 137CS along the northern edge of the Kuroshio Extension than expected from the observation, resulting the negative perturbations in both of the atmospheric and ocean parameters around 36° N, 146° E (Fig. 6O-2 and A-2). The concentration map of JCOPE-T-2-C (Fig. 7a) suggests that the concentration caused by the direct release is almost limited in the shelf region and the observed concentration in open ocean might be caused by the atmospheric deposition at the

Inverse estimation of source parameters of oceanic radioactivity dispersion models

Y. Miyazawa et al.

Title Page

Abstract

Introduction

Conclusions

References

Tables

Figures



Back

Close

Full Screen / Esc

Printer-friendly Version

Interactive Discussion



time of the last week of April 2011. This is also supported by the contribution rates of JCOPE-T-2-C (Fig. 6O-1 and A-1) showing the positive (negative) perturbations of the atmospheric (ocean) parameter in open ocean. The optimized positive perturbation of the ocean parameter in JCOPE-T-2-C is basically determined by the response to the observations near the coast (Fig. 6O-1), which also contribute to the positive perturbation of the atmospheric parameter (Fig. 6A-1).

All four cases of JCOPE-T indicate similar estimates of the total amount of the direct release: 5.5–5.9 PBq but comparatively broad range of the estimate of the atmospheric deposition: 1.2–9.7 PBq (Table 3). The reason is that the former (latter) parameter is basically determined by the observations near the coast (the observations in both of coastal and open seas) as shown in Fig. 6O-1 and A-1. The smaller estimates of the atmospheric parameter in JCOPE-T-1 could be related to the unrealistic representation of the open sea currents and then could be rejected. The variation of ^{137}Cs near the coast mainly driven by the wind forced current (Miyazawa et al., 2012) is not much sensitive to the change of the nudging parameter, which generally affects the open sea condition (Sect. 2.1), and the detailed shape of the time sequences of the direct release flux. The estimated total amounts of the direct release thus exhibit a convergent result among JCOPE-T-1 and JCOPE-T-2 models (Table 3).

Figures 8 and 9 depict sequences of the weekly mean concentration of the simulation of JCOPE-T-2-C using the optimized parameters with the smallest expected cost function value (207 099) shown in Table 3. The cost function value of this simulation, 207 967, is quite similar to the expected value (207 099), suggesting the effectiveness of the Green's function approach in the optimization of these parameters. The observed concentration along 141.4°E in March 2011 (Fig. 8a, b) is actually reproduced by the inclusion of the atmospheric deposition flux even though the model still underestimates it. The horizontal distribution near FNPP in the last half of April is basically governed by the direct release flux because Fig. 8b–d is qualitatively similar to Fig. 5b–d, respectively. The wider scale distribution in open ocean is significantly affected by the atmospheric deposition flux throughout the target period as shown in Fig. 9. The observed

Inverse estimation of source parameters of oceanic radioactivity dispersion models

Y. Miyazawa et al.

Title Page

Abstract

Introduction

Conclusions

References

Tables

Figures



Back

Close

Full Screen / Esc

Printer-friendly Version

Interactive Discussion



Inverse estimation of source parameters of oceanic radioactivity dispersion models

Y. Miyazawa et al.

Title Page

Abstract

Introduction

Conclusions

References

Tables

Figures

⏪

⏩

◀

▶

Back

Close

Full Screen / Esc

Printer-friendly Version

Interactive Discussion



anomalous concentration in open ocean during this period is considered to originate from the atmospheric deposition. The optimized parameters allow to represent time sequences of ^{137}Cs variations near FNPP: in front of FNPP, in front of Fukushima Daini nuclear power plant (10 km south of FNPP), and the Iwasawa Coast (16 km south of FNPP), as observed (Fig. 10), though the peak magnitude of the observation in front of FNPP (Fig. 10a) is not completely reproduced due to the coarse grid ($1/36^\circ$) of the model. The simulation assuming a flat shape of the CRIEPI type flux sequence during the period from 26 March to 6 April 2011 (Fig. 4) reproduces two peaks of the observation in April 2011 as shown in Fig. 10a and results in the smallest cost function value among the all simulations after the parameters optimization (Table 3), suggesting that the ^{137}Cs variation in front of FNPP is basically caused by not the direct release flux but the ocean current variation as mentioned by Tsumune et al. (2012).

The previous studies of the ocean dispersion simulations associated with the Fukushima accident (Kawamura et al., 2011; Tsumune et al., 2012) report 4 PBq for the period from 21 March to 30 April (Kawamura et al., 2011) and 3.5 ± 0.7 PBq for the period from 26 March to 31 May (Tsumune et al., 2012) of the ^{137}Cs total direct release amount. Their estimates are based on only the observations in front of FNPP (the 5th–6th and south discharge canal waters), while our estimates utilize all available observations except for the observations in front of FNPP, which may be not well represented by the comparatively coarse grid ($1/36^\circ$ and $1/12^\circ$) used for our simulation models. However, our larger estimate of the direct release flux, 5.5–5.9 PBq for the period from 21 March to 6 May 2011, succeeds to reproduce the ^{137}Cs variations observed along the coast (Fig. 10b, c) though the other model underestimates them (Fig. 11 of Tsumune et al., 2012). The simulation presented by Kawamura et al. (2011) seems to well reproduce them (their Fig. 2) but their simulation represents more enhanced southward dispersion along the coast than our simulations (Masumoto et al., 2012). The difference of estimated total amounts of the direct release among different studies could be attributed to possible differences in the model configurations and acceptable for better understanding to uncertainty of the source information.

models. The down-scaled model reasonably represents the contrast of the dispersions near FNPP dominantly governed by the direct release and in open ocean basically determined by the atmospheric dispersion, resulting in the plausible estimate of the total amounts of both the direct release and atmospheric dispersion. The basin-scale model could be used for the estimation of the total amount of the atmospheric deposition widely spread over the Western North Pacific.

Acknowledgements. This work is part of the Japan Coastal Ocean Predictability Experiment (JCOPE) promoted by the Japan Agency for Marine-Earth Science and Technology (JAM-STE). The authors wish to thank the numerical modeling subgroup of the Oceanographic Society of Japan led by Motoyoshi Ikeda for many useful suggestions. The authors would also like to thank the fruitful discussions with Daisuke Tsumune, Michio Aoyama, and Takuya Kobayashi.

References

- Aoyama, M., Igarashi, Y., and Hirose, K.: Learning from the monthly measurement of the fallout during 660 months – ^{90}Sr , ^{137}Cs , and Pu fallouts from April 1957 to March 2012, *Sci. J. KAGAKU*, 82, 442–457, 2012a (in Japanese).
- Aoyama, M., Tsumune, D., and Hamajima, Y.: Distribution of ^{137}Cs and ^{134}Cs in the North Pacific Ocean: impacts of the TEPCO Fukushima-daiichi NPP accident, *J. Radioanal. Nucl. Ch.*, doi:10.1007/s10967-012-2033-2, in press, 2012b.
- Bailly du Bois, P., Laguionie, P., Boust, D., Korsakissok, I., Didier, D., and Fievet, B.: Estimation of marine source-term following Fukushima Dai-ichi accident, *J. Environ. Radioact.*, 114, 2–9, doi:10.1016/j.jenvrad.2011.11.015, 2012.
- Buesseler, K., Aoyama, M., and Fukasawa, M.: Impacts of the Fukushima nuclear power plants on marine radioactivity, *Environ. Sci. Technol.*, 45, 9931–9935, doi:10.1021/es202816c, 2011.
- Chino, M., Nakayama, H., Nagai, H., Terada, H., Katata, G., and Yamazawa, H.: Preliminary estimation of release amounts of ^{131}I and ^{137}Cs accidentally discharged from the Fukushima Daiichi nuclear power plant into the atmosphere, *J. Nucl. Sci. Technol.*, 48, 1129–1134, 2011.

Inverse estimation of source parameters of oceanic radioactivity dispersion models

Y. Miyazawa et al.

Title Page

Abstract

Introduction

Conclusions

References

Tables

Figures



Back

Close

Full Screen / Esc

Printer-friendly Version

Interactive Discussion



Inverse estimation of source parameters of oceanic radioactivity dispersion models

Y. Miyazawa et al.

Title Page

Abstract

Introduction

Conclusions

References

Tables

Figures

◀

▶

◀

▶

Back

Close

Full Screen / Esc

Printer-friendly Version

Interactive Discussion



Conkright, M. E., Antonov, J. I., Baranova, O., Boyer, T. P., Garcia, H. E., Gelfeld, R., Johnson, D., Locarnini, R. A., Murphy, P. P., O'Brien, T. D., Smolyar, I., and Stephens, C.: World Ocean Database 2001, vol. 1, Introduction, edited by: Levitus, S., NOAA Atlas NESDIS 42, US Government Printing Office, Washington DC, 167 pp., 2002.

Guo, X., Varlamov, S. M., and Miyazawa, Y.: Coastal ocean modeling by nesting method, *Bull. Coast. Oceanogr.*, 47, 113–123, 2010 (in Japanese).

Honda, M., Aono, T., Aoyama, M., Hamajima, Y., Kawakami, H., Kitamura, M., Masumoto, Y., Miyazawa, Y., Takigawa, M., and Saino, T.: Dispersion of artificial caesium-134 and -137 in the Western North Pacific one month after the Fukushima accident, *Geochem. J.*, 46, 1–9, 2012.

Kagimoto, T., Miyazawa, Y., Guo, X., and Kawajiri, H.: High resolution Kuroshio forecast system – description and its applications, in: High Resolution Numerical Modeling of the Atmosphere and Ocean, edited by: Ohfuchi, W. and Hamilton, K., Springer, New York, 209–234, 2008.

Kalnay, E., Kanamitsu, M., Kistler, R., Collins, W., Deaven, D., Gandin, L., Iredell, M., Saha, S., White, G., Woollen, J., Zhu, Y., Leetmaa, A., Reynolds, R., Chelliah, M., Ebisuzaki, W., Higgins, W., Janowiak, J., Mo, K. C., Ropelewski, C., Wang, J., Jenne, R., and Joseph, D.: The NCEP/NCAR 40-year reanalysis project, *B. Am. Meteorol. Soc.*, 77, 437–471, 1996.

Kawamura, H., Kobayashi, T., Furuno, A., In, T., Ishikawa, Y., Nakayama, T., Shima, S., and Awaji, T.: Preliminary numerical experiments on oceanic dispersion of ^{131}I and ^{137}Cs discharged into the ocean because of the Fukushima daiichi nuclear power plant disaster, *J. Nucl. Sci. Technol.*, 48, 1349–1356, 2011.

Li, Y., Gao, Z., Lenschow, D. H., and Chen, F.: An improved approach for parameterizing surface-layer turbulent transfer coefficients in numerical models, *Bound.-Lay. Meteorol.*, 137, 153–165, 2010.

Maryon, R. H., Saltbones, J., Ryall, D. B., Bartnicki, J., Jakobsen, H. A., and Berge, E.: An intercomparison of three long range dispersion models developed for the UK meteorological office, DNMI and EMEP, UK Met Office Turbulence and Diffusion, Note 234, 44 pp., 1996.

Masumoto, Y., Miyazawa, Y., Tsumune, D., Kobayashi, T., Estournel, C., Marsaleix, P., Lanerolle, L., Mehra, A., and Garraffo, Z. D.: Oceanic dispersion simulation of Cesium 137 from Fukushima Daiichi Nuclear Power Plant, *Elements*, 8, 207–212, 2012.

Matsumoto, K., Takanezawa, T., and Ooe, M.: Ocean tide models developed by assimilating TOPEX/POSEIDON altimeter data into hydrodynamical model: a global model and a regional model around Japan, *J. Oceanogr.*, 56, 567–581, 2000.

Inverse estimation of source parameters of oceanic radioactivity dispersion models

Y. Miyazawa et al.

Title Page

Abstract

Introduction

Conclusions

References

Tables

Figures

◀

▶

◀

▶

Back

Close

Full Screen / Esc

Printer-friendly Version

Interactive Discussion



- Menemenlis, D., Fukumori, I., and Lee, L.: Using Green's functions to calibrate an ocean general circulation model, *Mon. Weather Rev.*, 133, 1224–1240, 2005.
- Ministry of Education, Culture, Sports, Science and Technology (MEXT): Monitoring information of environmental radioactivity level, available at: <http://radioactivity.mext.go.jp/en/> (last access: 10 October 2012), 2011.
- 5 Miyazawa, Y., Zhang, R., Guo, X., Tamura, H., Ambe, D., Lee, J.-S., Okuno, A., Yoshinari, H., Setou, T., and Komatsu, K.: Water mass variability in the Western North Pacific detected in a 15-year eddy resolving ocean reanalysis, *J. Oceanogr.* 65, 737–756, 2009.
- Miyazawa, Y., Masumoto, Y., Varlamov, S. M., and Miyama, T.: Transport simulation of the radionuclide from the shelf to open ocean around Fukushima, *Cont. Shelf Res.*, doi:10.1016/j.csr.2012.09.002, in press, 2012.
- 10 Morino, Y., Ohara, T., and Nishizawa, M.: Atmospheric behavior, deposition, and budget of radioactive materials from the Fukushima Daiichi nuclear power plant in March 2011, *Geophys. Res. Lett.*, 38, L00G11, doi:10.1029/2011GL048689, 2011.
- 15 Nuclear Emergency Response Headquarters (NERH), Government of Japan: Report of the Japanese Government to the IAEA Ministerial Conference in Nuclear Safety – The accident at TEPCO's Fukushima Nuclear Power Stations, 7 June, available at: <http://www.iaea.org/newscenter/focus/fukushima/japan-report/> (last access: 10 October 2012), 2011.
- Oura, Y. and Ebihara, M.: Radioactivity concentrations of ^{131}I , ^{134}Cs and ^{137}Cs in river water in the greater Tokyo metropolitan area after the Fukushima Daiichi nuclear power plant accident, *Geochem. J.*, 46, 303–309, 2012.
- 20 Saito, K., Aranam, K., Hara, T., Segawa, T., Narita, M., and Honda, Y.: Nonhydrostatic atmospheric models and operational development at JMA, *J. Meteor. Soc. Jpn. B*, 85, 271–304, 2007.
- 25 Stohl, A., Seibert, P., Wotawa, G., Arnold, D., Burkhart, J. F., Eckhardt, S., Tapia, C., Vargas, A., and Yasunari, T. J.: Xenon-133 and caesium-137 releases into the atmosphere from the Fukushima Dai-ichi nuclear power plant: determination of the source term, atmospheric dispersion, and deposition, *Atmos. Chem. Phys.*, 12, 2313–2343, doi:10.5194/acp-12-2313-2012, 2012.
- 30 Takemura, T., Nakamura, H., Takigawa, M., Kondo H., Satonuma, T., Miyasaka, T., and Nakajima, T.: A numerical simulation of global transport of atmospheric particles emitted from the Fukushima Daiichi nuclear power plant, *Scientific Online Letters on the Atmosphere*, 7, 101–104, doi:10.2151/sola.2011-026, 2011.

Tokyo Electric Power Corporation (TEPCO): Detection of radioactive materials from the seawater around the discharge canal of Fukushima Daiichi Nuclear Power Station, Press Release 22 March, available at: <http://www.tepco.co.jp/en/press/corp-com/release/11032201-e.html> (last access: 10 October 2012), 2011.

- 5 Tsumune, D., Tsubono, T., Aoyama, M., and Hirose, K.: Distribution of oceanic ^{137}Cs from the Fukushima Dai-ichi Nuclear Power Plant simulated numerically by a regional ocean model, *J. Environ. Radioactiv.*, 111, 100–108, 2012.

BGD

9, 13783–13816, 2012

Inverse estimation of source parameters of oceanic radioactivity dispersion models

Y. Miyazawa et al.

Title Page

Abstract

Introduction

Conclusions

References

Tables

Figures

⏪

⏩

◀

▶

Back

Close

Full Screen / Esc

Printer-friendly Version

Interactive Discussion



Inverse estimation of source parameters of oceanic radioactivity dispersion models

Y. Miyazawa et al.

Title Page

Abstract

Introduction

Conclusions

References

Tables

Figures

⏪

⏩

◀

▶

Back

Close

Full Screen / Esc

Printer-friendly Version

Interactive Discussion



Table 1. Information of ^{137}Cs observation data obtained for the period from 21 March to 6 May 2011 (total amount: 417 samples).

Name	Number of points	Error (Bq l^{-1})	Detection limit (Bq l^{-1})	Reference
TEPCO	18	5	15	TEPCO (2011), Buesseler et al. (2011)
MEXT	12	3.3	10	MEXT (2011), Buesseler et al. (2011)
MIRAI ^a	29	0.005–0.001	0.002	Honda et al. (2012)
TANSEI ^{a,c}	21	0.09	0.12	Aoyama et al. (2012a)
NYK ^{b,c}	72	0.06–0.0002	0.0004	Aoyama et al. (2012a)
Oarai	5	3	9	Oarai Town ^d

^a The MIRAI and TANSEI data were sampled by the research cruises.

^b The NYK data were sampled through volunteer ships cruises managed by Nippon Yusen Kabushiki Kaisha (NYK LINE).

^c Data are available from http://www.mri-jma.go.jp/Topics/hotyouhi/houtyouhi_sea_en.html.

^d Data are available from http://www.town.oarai.lg.jp/~kouhitsu/housyasenn/info.g_3_1351.html (in Japanese).

Inverse estimation of source parameters of oceanic radioactivity dispersion models

Y. Miyazawa et al.

Title Page

Abstract

Introduction

Conclusions

References

Tables

Figures

◀

▶

◀

▶

Back

Close

Full Screen / Esc

Printer-friendly Version

Interactive Discussion

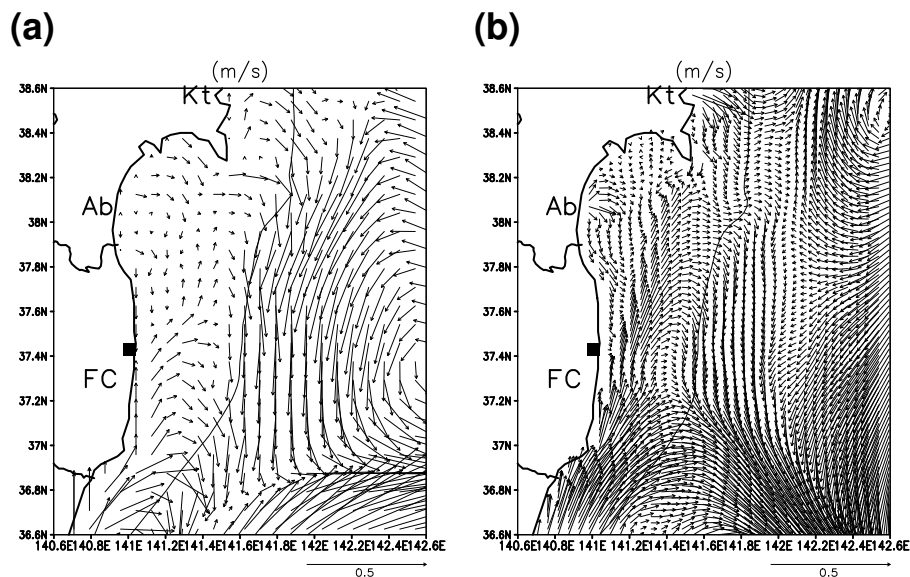


Fig. 1. Simulated ocean current at 1m depth averaged for the period from 21 March 2011 to 6 May 2011. A thick line denotes an iso-depth contour showing 200 m depth. A closed square indicates the position of FNPP. Abbreviations: “Ab”, “Kt”, and “FC” indicate the river mouth positions of the Abukuma and Kitakami rivers, and Fukushima coast, respectively. **(a)** JCOPE2 **(b)** JCOPE-T-2.

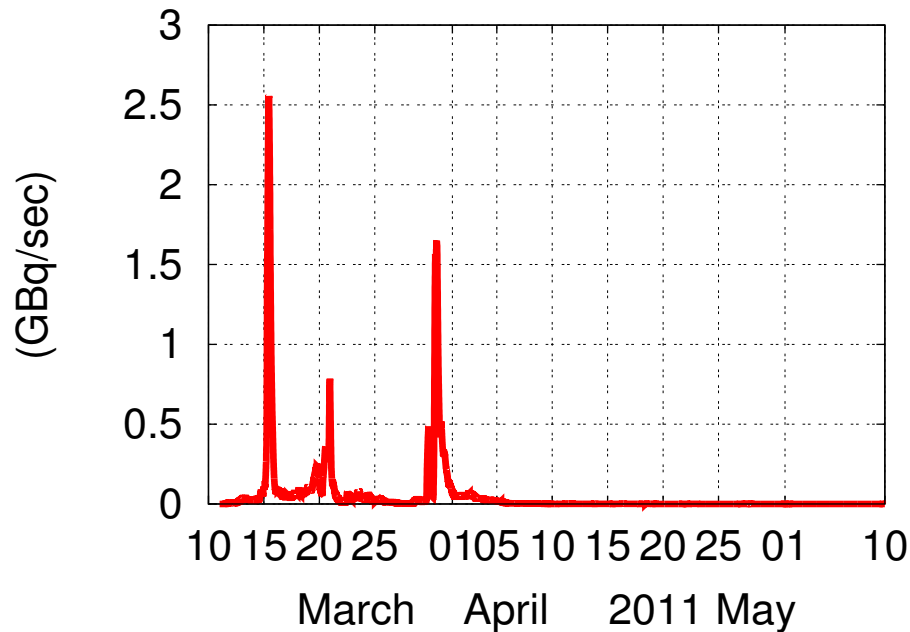


Fig. 2. Time sequences of the simulated atmospheric deposition flux (in GBq s^{-1}) integrated over the Western North Pacific, $10.5\text{--}62^\circ \text{N}$ and $108\text{--}180^\circ \text{E}$.

Inverse estimation of source parameters of oceanic radioactivity dispersion models

Y. Miyazawa et al.

Title Page

Abstract Introduction

Conclusions References

Tables Figures

⏪ ⏩

◀ ▶

Back Close

Full Screen / Esc

Printer-friendly Version

Interactive Discussion



Inverse estimation of source parameters of oceanic radioactivity dispersion models

Y. Miyazawa et al.

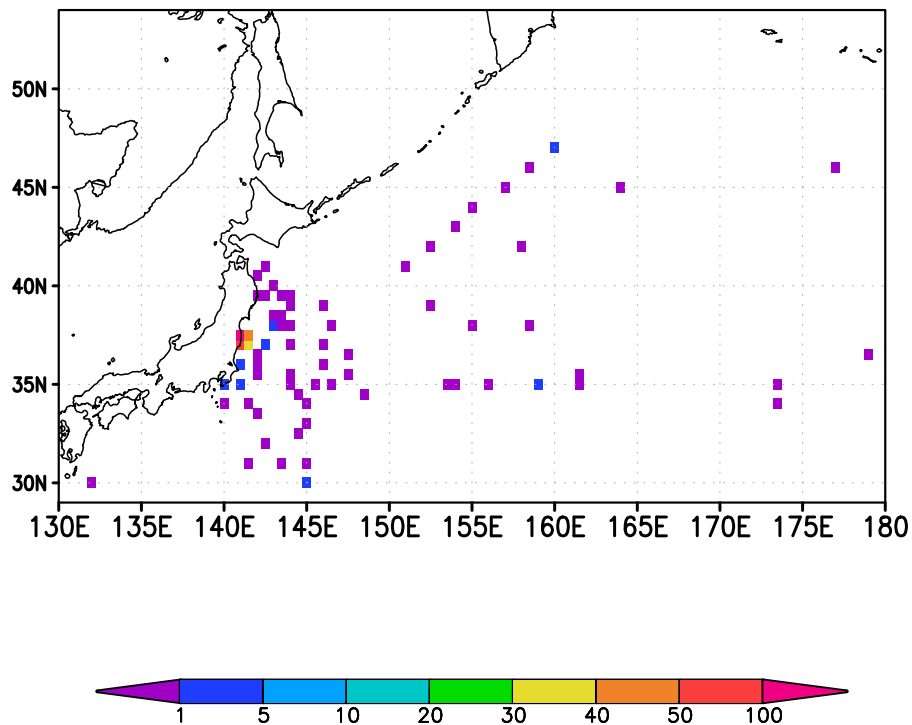


Fig. 3. Numbers of the caesium-137 (^{137}Cs) measurements within $1^\circ \times 1^\circ$ grids sampled during the period from 21 March to 6 May 2011.

[Title Page](#)[Abstract](#)[Introduction](#)[Conclusions](#)[References](#)[Tables](#)[Figures](#)[◀](#)[▶](#)[◀](#)[▶](#)[Back](#)[Close](#)[Full Screen / Esc](#)[Printer-friendly Version](#)[Interactive Discussion](#)

Inverse estimation of source parameters of oceanic radioactivity dispersion models

Y. Miyazawa et al.

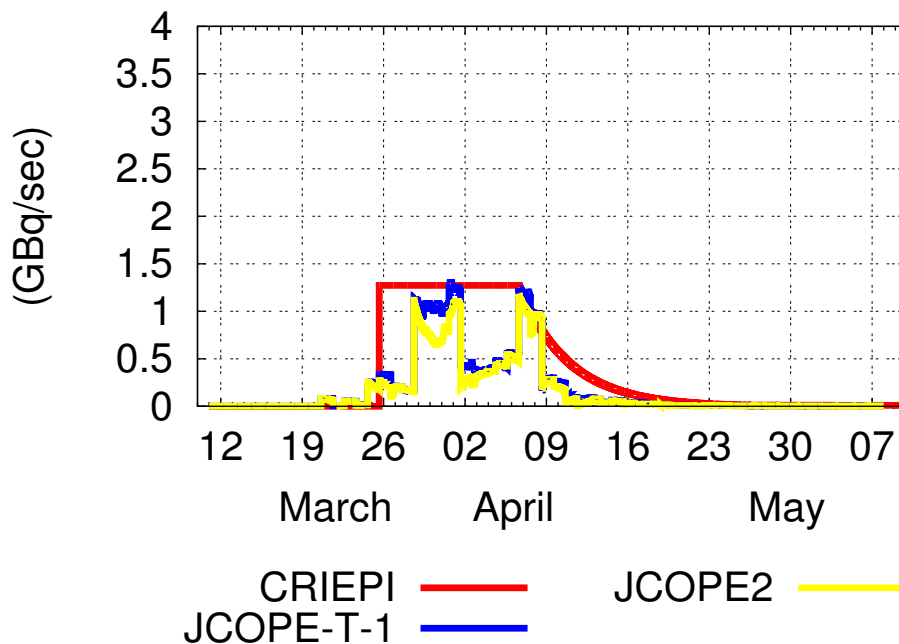


Fig. 4. Time sequences of the first guess direct release fluxes.

Title Page

Abstract Introduction

Conclusions References

Tables Figures

⏪ ⏩

◀ ▶

Back Close

Full Screen / Esc

Printer-friendly Version

Interactive Discussion

Inverse estimation of source parameters of oceanic radioactivity dispersion models

Y. Miyazawa et al.

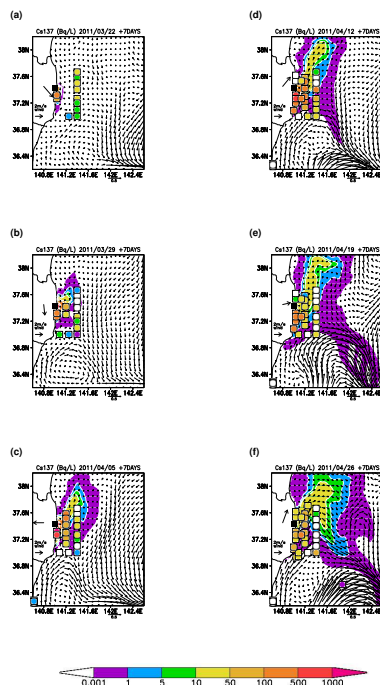


Fig. 5. Time sequences of weekly averaged concentration (in Bq l^{-1}) at 1 m depth (shade) of ^{137}Cs around Fukushima simulated by the JCOPE-T-2-C first guess simulation. Vectors indicate the weekly averaged current at 1 m depth used for the simulation. The beginning days of the weekly averages are shown at top of panels. The position of FNPP is denoted by a closed square. Closed circles surrounded by open squares indicate in-situ observation points during each averaged period. Colors of the closed circles denote ranges of the concentration. White color means that the concentration was not detected there. A vector shown in left of the FNPP point indicates the weekly averaged wind of JMA MSM on a grid in front of FNPP.

Title Page

Abstract

Introduction

Conclusions

References

Tables

Figures

◀

▶

◀

▶

Back

Close

Full Screen / Esc

Printer-friendly Version

Interactive Discussion

Inverse estimation of source parameters of oceanic radioactivity dispersion models

Y. Miyazawa et al.

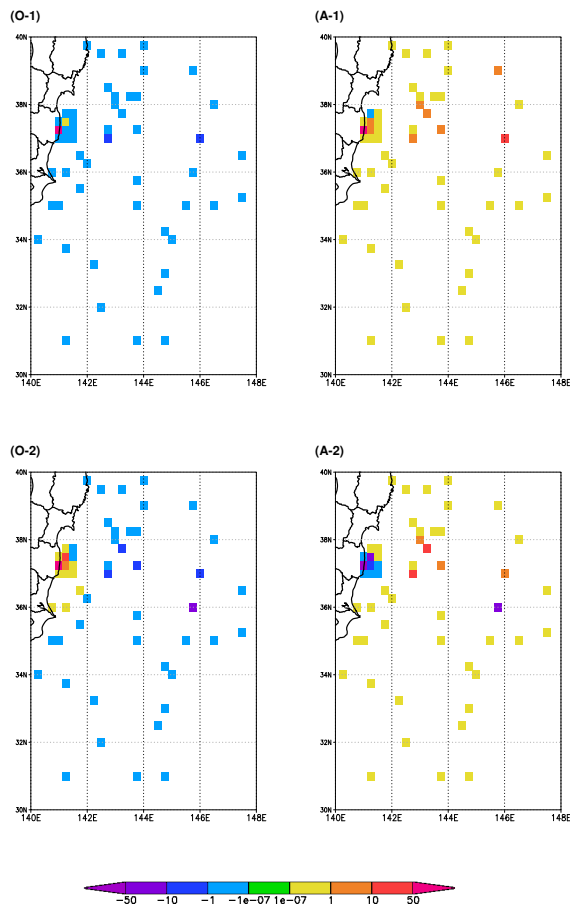


Fig. 6. Contribution rates (in %; Eq. 9) averaged in $1/4^\circ \times 1/4^\circ$ grids. **(O-1)** The ocean parameter in the JCOPE-T-2-C case. **(A-1)** The atmospheric parameter in the JCOPE-T-2-case. **(O-2)** As in **(O-1)** except for the JCOPE2 case. **(A-2)** as in **(A-1)** except for the JCOPE2 case.

[Title Page](#)
[Abstract](#)
[Introduction](#)
[Conclusions](#)
[References](#)
[Tables](#)
[Figures](#)
[⏪](#)
[⏩](#)
[◀](#)
[▶](#)
[Back](#)
[Close](#)
[Full Screen / Esc](#)
[Printer-friendly Version](#)
[Interactive Discussion](#)

Inverse estimation of source parameters of oceanic radioactivity dispersion models

Y. Miyazawa et al.

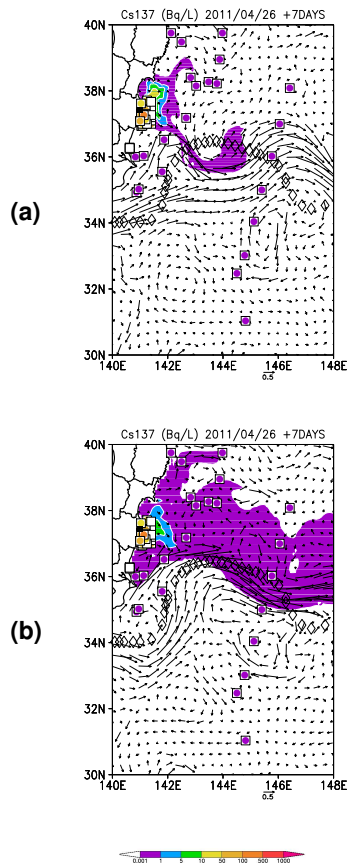


Fig. 7. (a) As in Fig. 5f except for showing wider region and with open diamonds indicating the position of the Kuroshio Extension front provided from Japan Coast Guard. **(b)** As in Fig. 7a except for the JCOPE2 first guess simulation.

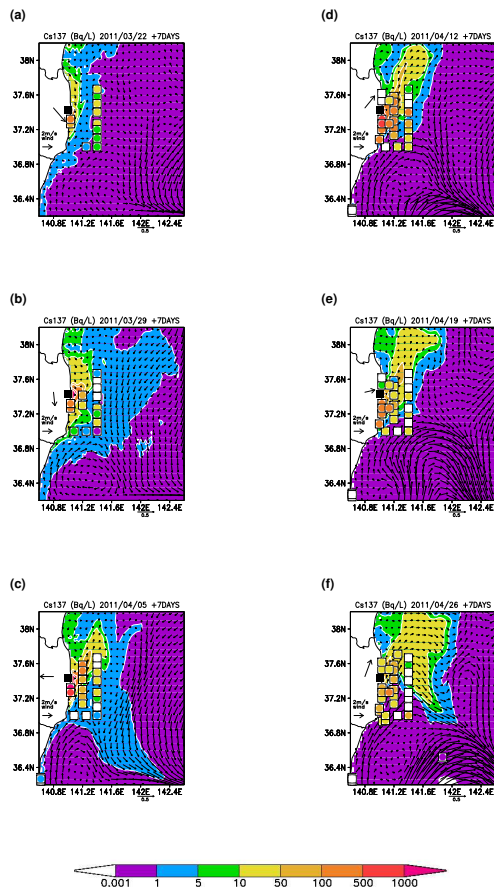


Fig. 8. As in Fig. 5 except for the JCOPE-T-2-C-E case.

Inverse estimation of source parameters of oceanic radioactivity dispersion models

Y. Miyazawa et al.

Title Page	
Abstract	Introduction
Conclusions	References
Tables	Figures
◀	▶
◀	▶
Back	Close
Full Screen / Esc	
Printer-friendly Version	
Interactive Discussion	



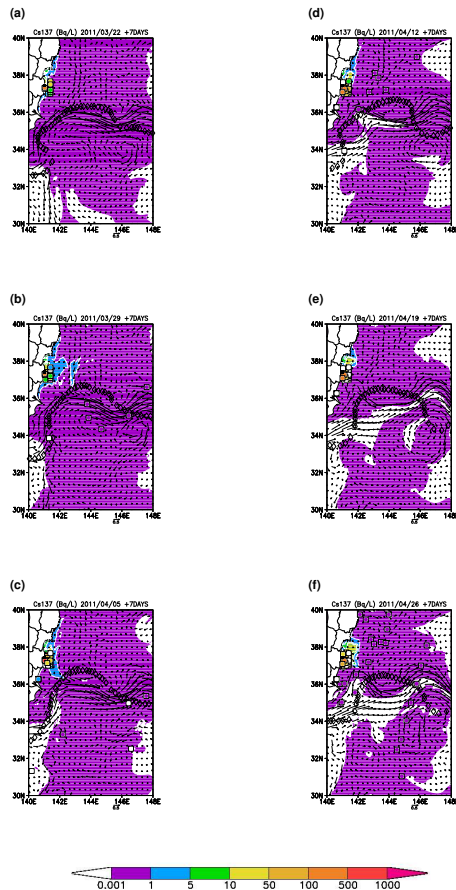


Fig. 9. As in Fig. 8 except for showing wider region and with open diamonds indicating the position of the Kuroshio Extension front provided from Japan Coast Guard.

Inverse estimation of source parameters of oceanic radioactivity dispersion models

Y. Miyazawa et al.

Title Page

Abstract Introduction

Conclusions References

Tables Figures

◀ ▶

◀ ▶

Back Close

Full Screen / Esc

Printer-friendly Version

Interactive Discussion



Inverse estimation of source parameters of oceanic radioactivity dispersion models

Y. Miyazawa et al.

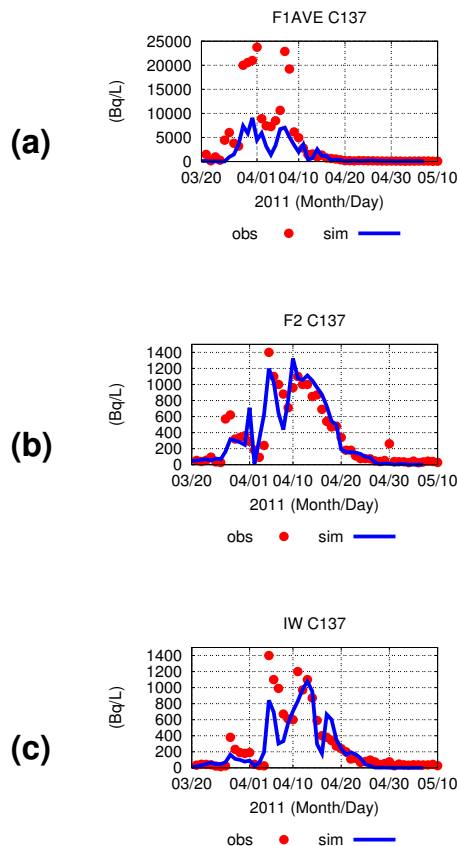


Fig. 10. Time sequences (curves) of ^{137}Cs at 1m depth on the points along the Fukushima coast simulated by the JCOPE-T-2-C-E case. Closed circles denote the observation at the corresponding points. **(a)** In front of FNPP. Closed circles denote the average of the measurements at two positions of the 5th–6th and south discharge canal waters. **(b)** In front of Fukushima Daini nuclear power plant (10 km south of FNPP). **(c)** The Iwasawa Coast (16 km south of FNPP).